Title

Solution NMR structure of Se0862, a highly conserved cyanobacterial protein involved in biofilm formation

Journal

Protein Science, 29(11)

ISSN

0961-8368

Authors

Zhang, Ning
Chang, Yong-Gang
Tseng, Roger
et al.

Publication Date

2020-11-01

DOI

10.1002/pro.3952

Peer reviewed

Received: 29 July 2020 | Revised: 8 September 2020 | Accepted: 12 September 2020

DOI: 10.1002/pro.3952

PROTEIN STRUCTURE REPORTS

THE PROTEIN SOCIETY WILEY

Solution NMR structure of Se0862, a highly conserved cyanobacterial protein involved in biofilm formation

Ning Zhang[1] | **Yong-Gang Chang**[1,7] | **Roger Tseng**[1,6] | **Sergey Ovchinnikov**[2] | **Rakefet Schwarz**[4] | **Andy LiWang**[1,3,5]

[1]Department of Chemistry and Chemical Biology, University of California, Merced, California

[2]Harvard University, Cambridge, Massachusetts

[3]Center for Cellular and Biomolecular Machines, University of California, Merced, California

[4]The Mina and Everard Goodman Faculty of Life Sciences, Bar-Ilan University, Ramat-Gan, Israel

[5]Health Sciences Research Institute, University of California, Merced, California

[6]United States Department of Agriculture, Ames, IA

[7]Monash University, Victoria, Australia

Correspondence
Andy LiWang, Department of Chemistry and Chemical Biology, University of California, Merced, CA 95343, USA.
Email: aliwang@ucmerced.edu

Funding information
Air Force Office of Scientific Research, Grant/Award Number: FA9550-17-1-0447; National Science Foundation, Grant/Award Number: NSF-HRD-1547848

Abstract

Biofilms are accumulations of microorganisms embedded in extracellular matrices that protect against external factors and stressful environments. Cyanobacterial biofilms are ubiquitous and have potential for treatment of wastewater and sustainable production of biofuels. But the underlying mechanisms regulating cyanobacterial biofilm formation are unclear. Here, we report the solution NMR structure of a protein, Se0862, conserved across diverse cyanobacterial species and involved in regulation of biofilm formation in the cyanobacterium *Synechococcus elongatus* PCC 7942. Se0862 is a class α+β protein with ααββββαα topology and roll architecture, consisting of a four-stranded β-sheet that is flanked by four α-helices on one side. Conserved surface residues constitute a hydrophobic pocket and charged regions that are likely also present in Se0862 orthologs.

KEYWORDS

biofilm, cyanobacteria, NMR spectroscopy, protein structure, *S. elongatus* PCC 7942

1 | INTRODUCTION

Cyanobacteria, also referred to as blue-green algae, are ancient photosynthetic organisms and the only prokaryotes known to carry out oxygenic photosynthesis, thrive in a wide range of ecological habitats, and can produce biofilms under certain conditions. Biofilms are communities of microorganisms that are enclosed in extracellular polymeric matrices that provide protection against toxic compounds and stressful environmental factors such as extreme temperatures and pH.[1] Biofilms from cyanobacteria have been used for wastewater treatment, research of sustainable biofuels and biological by-products, and soil fertility improvement.[2–12] In spite of these advantages, they can also be responsible for biodeterioration and biofouling that cause economic loss.[13–15]

Recently, there have been advances in understanding biofilm formation by cyanobacteria. For example, four small secreted proteins, EbfG1-4 (enable biofilm formation with GG-motif), of *S. elongatus* PCC 7942 have been found to promote biofilm-formation.[16,17] Also, *Synechocystis* sp. PCC 6803 mutants lacking type IV pili

(T4P) are unable to aggregate and form biofilms,[18] however, impairment of T4P formation in *S. elongatus* resulted in biofilm-forming-mutants, unlike the wild-type strain that grow planktonically.[19] These data suggest that *S. elongatus* and *Synechocystis* employ different mechanisms for biofilm development. T4P biogenesis is under the control of the circadian clock in cyanobacteria,[20] used for extension, adhesion, retraction and motility, and plays a role in natural transformation by pulling exogenous DNA close to the cell surface.[21,22]

Synpcc7942_0862 encodes a conserved hypothetical protein, Se0862, in *S. elongatus*, and its inactivation leads to biofilm development.[19] In order to gain insights into Se0862 as a biofilm regulator we cloned the gene, expressed it in *E. coli*, purified the protein, and determined the solution structure by NMR.

2 | RESULTS AND DISCUSSION

2.1 | NMR solution structure of Se0862

Purified Se0862 elutes from a preparative size-exclusion column as a monomer (Figure S1). A two-dimensional ^{1}H-^{15}N HSQC NMR spectrum of Se0862 obtained at a static magnetic field strength of 14.1 T is shown in Figure 1a. Standard heteronuclear triple resonance NMR experiments were used to assign backbone and sidechain

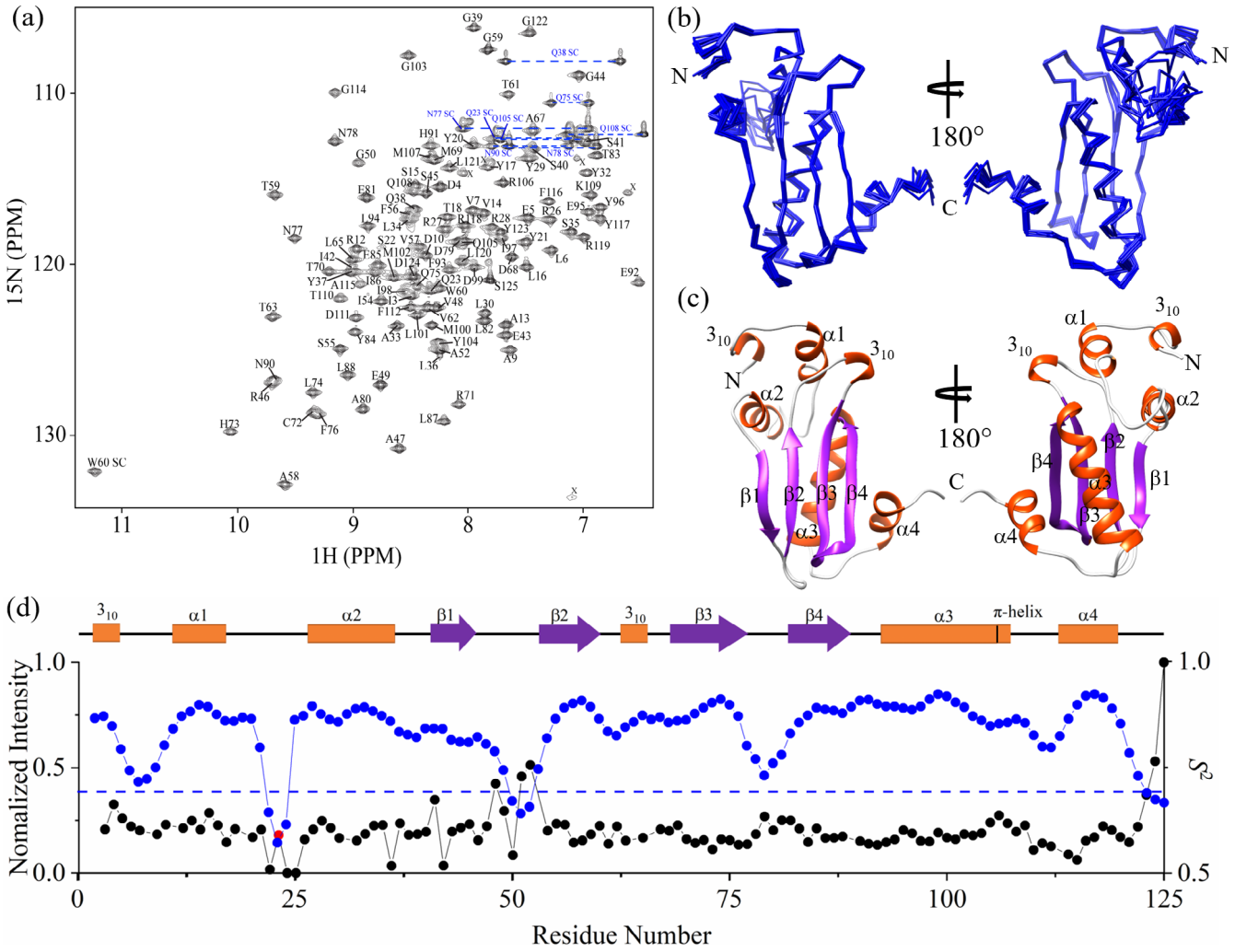

FIGURE 1 2D HSQC NMR spectrum and NMR solution structure of Se0862. (a) Assigned two dimensional ^{1}H-^{15}N HSQC spectrum of Se0862. SC, side chain. Blue dashed lines connect pairs of peaks of NH_2 groups of Asn and Gln side chains. Unassigned peaks are marked with an "x". (b) Superposition of backbone atoms of a family of 10 lowest-energy structures of Se0862. (c) Ribbon diagram of the energy-minimized average structure. (d) Plot of normalized ^{15}N,^{1}H HSQC peak intensities (black circles) and TALOS-calculated S^2 values (blue circles) as a function of residue number. Blue dash line represents S^2 value of 0.7. The backbone resonance of residue Q23 overlaps with that of W60 and is thus its intensity is denoted with a red circle. Resonances for A24 and N25 were unobservable and are thus assumed to have near-zero peak intensities

TABLE 1 Structural statistics for Se0862

Protein data Bank accession number	6UF2
BMRB accession number	30,676
Total residue number	125
NMR constraints	
Distance constraints	
Total	2045
Intra-residue	1,080
Inter-residue	
Sequential ($\|i–j\| = 1$)	553
Medium-range ($1 < \|i–j\| \leq 4$)	184
Long-range ($\|i–j\| > 4$)	228
Total dihedral angle restraints	192
Phi (ϕ)	96
Psi (ψ)	96
Total RDCs	175
HN-N	63
HA-CA	56
CA-CO	56
Q[a]	0.173
Structure statistics	
Violations (mean ± s.d.)	
Distance constraints (Å)	0.068 ± 0.056
Dihedral angle constraints (°)	0.893 ± 0.778
Dihedral angle violation (>5.0°)	0
Distance violation (>0.5 Å)	0
Deviation from idealized geometry	
Bond lengths (Å)	0.007 ± 0.000
Bond angle (°)	0.862 ± 0.016
Impropers (°)	0.573 ± 0.021
Average pairwise r.m.s.d. (Å)[b]	
Heavy atoms (all) (α-helices & β-strands)	0.85
Backbone atoms (all) (α-helices & β-strands)	0.25
Ramachandran plot (%)	
Richardson Lab's Molprobity	
Most favored regions	96.8
Allowed regions	3.2
Disallowed regions	0.0
PROCHECK	
Most favored regions	91.1
Additional allowed regions	7.4
Generously allowed regions	1.5
Disallowed regions	0.0

chemical shifts of 121 out of 125 residues. The four residues without any chemical shift assignments are M1, R2, A24, and N25. All nine prolyl residues—P8, P11, P19, P31, P53, P64, P66, P89, P113—adopt the *trans* conformation (Table S1), as based on differences between their $^{13}C^{\beta}$ and $^{13}C^{\gamma}$ chemical shifts[23] (range: 2.54–5.62 ppm; measured using the CC(CO)NH experiment[24]) and the program Promega.[25] The structure of Se0862 was calculated using XPLOR-NIH[26] with 2045 distance restraints, 192 ϕ, ψ backbone dihedral angle restraints determined by TALOS-N,[27] and 63 ^{15}N–H, 56 $^{13}C^{\alpha}$–H^{α}, and 56 $^{13}C^{\alpha}$–$^{13}C'$ residual dipolar coupling restraints. Figure 1b shows the family of the 10 lowest-energy structures out of 100. Statistics on the family of structures are listed in Table 1. There were no violations of NOE-derived distance restraints (threshold of 0.5 Å) or TALOS-derived dihedral angle restraints (threshold of 5°). The family of 10 structures of Se0862 is well-defined with a root-mean-square deviation (RMSD) of 0.25 Å for backbone atoms and 0.85 Å for all heavy atoms. The ribbon representation of the average minimized structure is shown in Figure 1c. Se0862 adopts an αααββββαα topology with two antiparallel N-terminal α-helices (α1: P11-Y17; α2: Y29-Y37), a four-stranded antiparallel β-sheet (β1: I42-K46; β2: I54-T59; β3: M69-Q75; β4: D79-P89), two antiparallel C-terminal α-helices (α3: N90-R106; α4: G114-L121), two 3_{10}-helices (I3-E5 and L65-A67) and a π-helix (Q105-R106)[28] (Figure 1c). According to CATH,[29] which is a database that classifies distinct globular domains into homologous superfamilies, Se0862 is a class α + β protein with roll architecture. Normalized ^{1}H-^{15}N HSQC peak intensities and order parameters, S^2, derived from chemical shifts[27,30] are plotted in Figure 1d and suggest that two type I turns between β1 and β2 and between β3 and β4 experience local dynamics on the fast time scale, whereas the loop between α1 and α2 also undergoes motions on the intermediate time scale.

2.2 | Structural properties and potential function of Se0862

The α-helices within each antiparallel pair pack together through mostly hydrophobic interactions, as do the

[a]Quality factor (or *Q* factor) is used to quantify the extent of agreement between a calculated structure and measured dipolar couplings. A *Q* factor below 0.2 can be used as a rule of thumb to indicate good agreement.
[b]For RMSD calculation, residues 13–18, 28–59, 69–107, 114–120 of Se0862 were used.

β-strands within the sheet. The helices pack against one face of the β-sheet through interactions between nonpolar side chains. The hydrophobicity and solvent accessible surface area (SASA) of residues were calculated using ProtScale[31] and GETAREA[32] tools, respectively, and show that almost all conserved hydrophobic residues are buried whereas charged residues tend to be solvent exposed (Figure 2a), as is to be expected.

Several nonpolar residues, including I42, F56, M100, and L101, form a hydrophobic pocket (Figure 2b), and because many of these residues are conserved (Figure S2), the structure of the pocket might be conserved as well. Also, there is a putative salt bridge between conserved residues E85 (β4) and R71 (β3) (Figure 2c). The electrostatic surface potential of Se0862, as calculated using the APBS tool in Chimera,[33] is shown in Figure 2b with conserved acidic and basic residues labeled. A negatively charged patch is formed by the following conserved residues: residues D68, E92, E95, and D99. Two positively charged patches—(a) R27, R28, and R46, and (b) R118 and R119—are also composed of conserved residues and are separated by the negatively charged patch. The total solvent accessible surface area is 8,640 Å^2 according to PDBePISA.[34]

Using Se0862 as query, PSI-BLAST identified 478 proteins with sequence identities over 40%, all from cyanobacteria, showing that Se0862 orthologs are widespread in these organisms. However, they are designated as hypothetical proteins and missing structural and functional information. A DALI[35,36] search of the Protein Data Bank identified 123 polypeptide chains with Z-scores above 2 but lower than 3.4 (Z-score > 2 suggests that

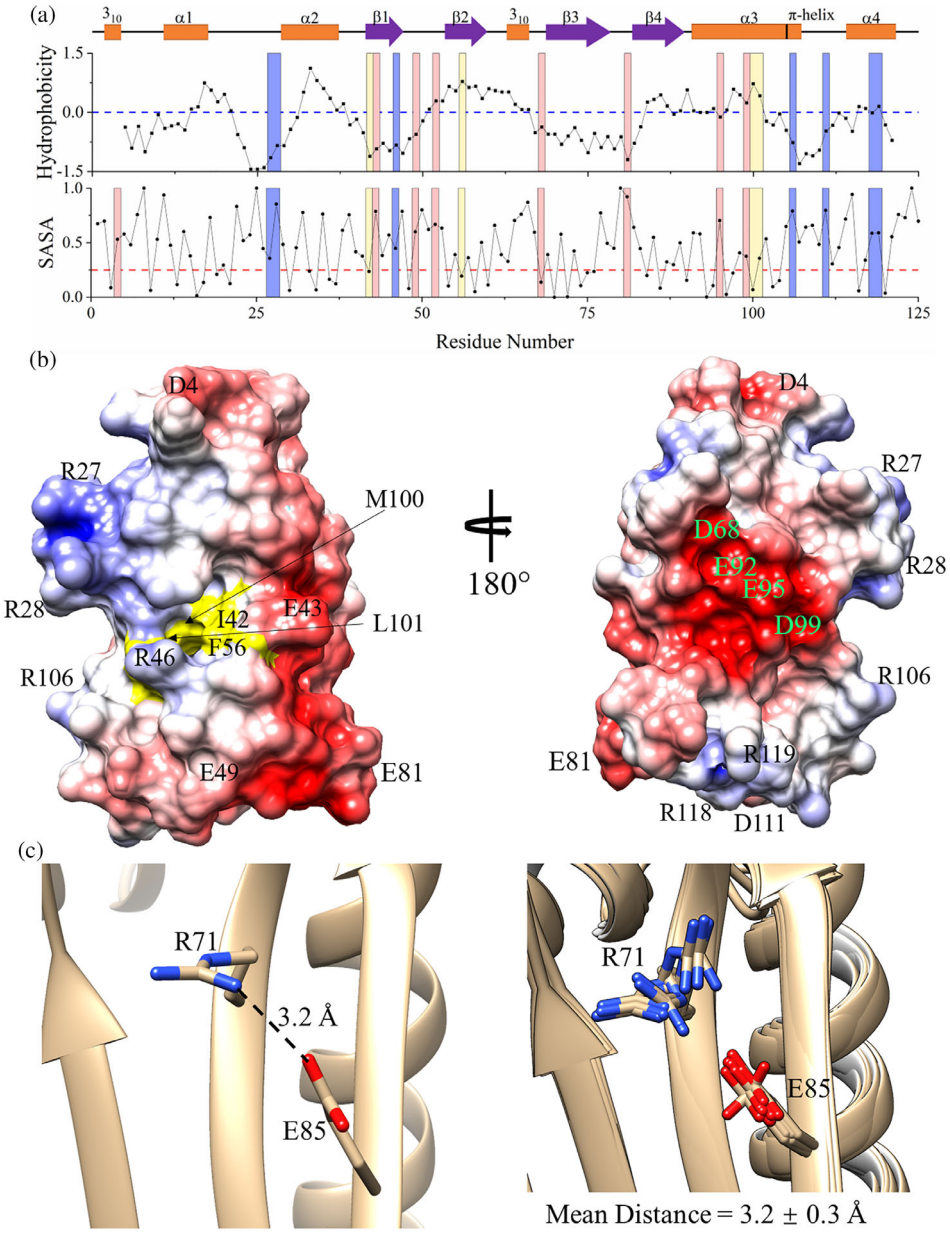

FIGURE 2 Surface properties of Se0862. (a) Hydrophobicity and SASA plots of Se0862 as a function of its primary sequence. Light yellow, red, and blue rectangles indicate conserved hydrophobic, acidic, and basic residues, respectively. Dashed horizontal lines represent 0 hydrophobicity and 0.25 SASA. (b) Hydrophobic pocket (rendered yellow) and electrostatic surface potential of Se0862 with conserved residues labeled. The scale for the surface potential is from $-5\ k_BT/e$ (red) to $+5\ k_BT/e$ (blue). (c) Side chains of E85 and R71 in the energy-minimized average structure (left) and 10 lowest-energy structures (right). The indicated distance is between an O^{ε} atom of E85 and an N^{η} atom of R71

structural similarity is significant). The top 20 DALI hits are listed in Table S2 but they did not provide clear insights into the likely function of Se0862.

Inactivation of Synpcc7942_0862 causes biofilm formation[19] and the protein encoded by this gene is also required for natural competence, the latter of which is known to need T4P.[20] A testable hypothesis is that the negatively and positively charged regions and hydrophobic pocket of Se0862 are sites of interaction with complementary sites on T4P components to regulate biofilm formation, pili biogenesis, and/or extension in cyanobacteria.

3 | MATERIALS AND METHODS

3.1 | NMR spectroscopy

All NMR experiments were carried out at a calibrated sample temperature of 22°C on a Bruker Avance III 600 MHz spectrometer equipped with a TCI cryoprobe. ^{1}H chemical shifts were referenced to internal 3-(trimethyl-silyl)-1-propanesulfonic acid sodium salt (DSS). ^{13}C and ^{15}N chemical shifts were indirectly referenced to DSS using absolute frequency ratios listed on the BMRB website. NMR samples contained ~0.6 mM ^{15}N/^{13}C-enriched protein in 350 μL NMR buffer (20 mM Tris, 100 mM NaCl, 5 mM TCEP, 0.02% NaN_3, 10 μM DSS, pH 7.0, 95% H_2O/5% D2O). 3D HNCACB, HN(CO)CACB, HNCO, HN(CA)CO, HBHA(CO)NH, HCCH(CO)NH, CC(CO)NH, (H)CCH-COSY, H(C)CH-COSY, (H)CCH-TOCSY experiments were used for backbone and aliphatic side-chain assignments[37]; 2D (HB)CB(CDCG)HG and (HB)CB(CDCGCE)HE experiments were acquired for aromatic side chain assignments.[38] 3D ^{15}N-edited, ^{13}C-edited NOESY-HSQC, and 4D ^{13}C /^{13}C-edited NOESY-HSQC spectra were collected for interproton distance restraints for structure determination. A chemical shift-based structural model of Se0862 generated by CS-ROSETTA was used to guide initial NOE assignments. Please see Table S3 for further details on NMR experiments. NMR data were processed with NMRPipe[39] and analyzed using NMRFAM-Sparky.[40] All details on cloning, expression and purification of Se0862 are presenting in supplementary materials.

3.2 | NMR structure calculations

Backbone dihedral angle restraints were predicted from backbone chemical shifts using TALOS-N.[27] All NOE distance restraints were grouped into four ranges (strong, medium, weak, very weak) according to NOE cross-peak intensities. The lower distance bound for all distance restraints was set to 1.8 Å. The upper bound was 2.7 Å for strong NOEs, 3.3 Å for medium NOEs, 5.0 Å for weak NOEs, and 6.0 Å for very weak NOEs. For methyl group NOEs an additional 0.5 Å was added to the upper bound of distance restraints. Structures were calculated with XPLOR-NIH.[26] During the high temperature stage of calculations, force constants for distances (k_{NOE}), dihedral angles (k_{CDIH}), torsion angles (k_{tDB}), implicit solvation (EEFx, k_{EEFx}), angles (k_{ANGL}), and improper torsions (k_{IMPR}) were 2 kcal mol^{-1} Å^{-2}, 10 kcal mol^{-1} Å^{-2}, 0.02 kcal mol^{-1} Å^{-2}, 0.1 kcal mol^{-1} Å^{-2}, 0.4 kcal mol^{-1} Å^{-2}, and 0.1 kcal mol^{-1} Å^{-2}, respectively. In the simulated annealing stage, k_{NOE}, k_{tDB}, k_{EEFx}, k_{ANGL}, and k_{IMPR} were gradually increased from 2 to 30 kcal mol^{-1} Å^{-2}, 0.1 to 1.0 kcal mol^{-1} rad^{-2}, 0.1 to 1.0 kcal mol^{-1} Å^{-2}, 0.4 to 1.0 kcal mol^{-1} rad^{-2}, and 0.1 to 1.0 kcal mol^{-1} Å^{-2}, respectively, and k_{CDIH} was set to 200 kcal mol^{-1} rad^{-2}. Temperature in the simulated annealing stage was decreased from 3,500 K to 25 K in steps of 12.5 K. Structure validation statistics were generated by the PSVS web server,[41] PROCHECK,[42] and MolProbity[43] (Table 1). Calculations of surface potential and hydrophobicity[44] and structural renderings were carried out by UCSF ChimeraX.[45] α-helices, β-strands, and 3_{10} and π-helices were identified using the "dssp report true" command in ChimeraX.

ACKNOWLEDGMENTS

This research was supported by grants from Air Force Office of Scientific Research (FA9550-17-1-0447) and NSF-CREST: Center for Cellular and Biomolecular Machines at the University of California, Merced (NSF-HRD-1547848). Molecular graphics and analyses performed with UCSF ChimeraX, developed by the Resource for Biocomputing, Visualization, and Informatics at the University of California, San Francisco, with support from National Institutes of Health R01-GM129325 and the Office of Cyber Infrastructure and Computational Biology, National Institute of Allergy and Infectious Diseases.

CONFLICT OF INTEREST

The authors declare no conflict of interest.

AUTHOR CONTRIBUTIONS

Ning Zhang: Data curation; formal analysis; investigation; methodology; writing-original draft; writing-review and editing. **Yong-Gang Chang:** Data curation; formal analysis; investigation; writing-review and editing. **Roger Tseng:** Data curation; formal analysis; investigation; writing-review and editing. **Sergey Ovchinnikov:** Formal analysis; investigation. **Rakefet Schwarz:**

Conceptualization; resources; writing-review and editing. **Andy LiWang:** Conceptualization; funding acquisition; project administration; supervision; writing-review and editing.

ORCID

Ning Zhang https://orcid.org/0000-0002-3590-3774
Andy LiWang https://orcid.org/0000-0003-4741-6946

REFERENCES

1. Flemming HC, Wingender J. The biofilm matrix. Nat Rev Microbiol. 2010;8:623–633.
2. Bruno L, Di Pippo F, Antonaroli S, Gismondi A, Valentini C, Albertano P. Characterization of biofilm-forming cyanobacteria for biomass and lipid production. J Appl Microbiol. 2012;113: 1052–1064.
3. Egan S, Thomas T, Kjelleberg S. Unlocking the diversity and biotechnological potential of marine surface associated microbial communities. Curr Opin Microbiol. 2008;11: 219–225.
4. Godlewska K, Michalak I, Pacyga P, Basladynska S, Chojnacka K. Potential applications of cyanobacteria: Spirulina platensis filtrates and homogenates in agriculture. World J Microbiol Biotechnol. 2019;35:80.
5. Ivnitsky H, Katz I, Minz D, et al. Bacterial community composition and structure of biofilms developing on nanofiltration membranes applied to wastewater treatment. Water Res. 2007; 41:3924–3935.
6. Lau NS, Matsui M, Abdullah AA. Cyanobacteria: Photoautotrophic microbial factories for the sustainable synthesis of industrial products. Biomed Res Int. 2015;2015:754934.
7. Liehr SK, Chen HJ, Lin SH. Metals removal by algal biofilms. Water Sci Technol. 1994;30:59–68.
8. Roeselers G, van Loosdrecht MCM, Muyzer G. Phototrophic biofilms and their potential applications. J Appl Phycol. 2008; 20:227–235.
9. Rossi F, De Philippis R. Role of cyanobacterial exopolysaccharides in phototrophic biofilms and in complex microbial mats. Life. 2015;5:1218–1238.
10. Singh R, Parihar P, Singh M, et al. Uncovering potential applications of cyanobacteria and algal metabolites in biology, agriculture and medicine: Current status and future prospects. Front Microbiol. 2017;8:515.
11. Wagner M, Loy A, Nogueira R, Purkhold U, Lee N, Daims H. Microbial community composition and function in wastewater treatment plants. Anton Leeuw Int J G. 2002;81:665–680.
12. Albertano P. Cyanobacterial biofilms in monuments and caves. In: Whitton BA, editor. Ecology of cyanobacteria II: Their diversity in space and time. Dordrecht, Netherlands: Springer, 2012; p. 317–343.
13. de Carvalho CCCR. Marine bio films: A successful microbial strategy with economic implications. Front Mar Sci. 2018; 5:126.
14. Scheerer S, Ortega-Morales O, Gaylarde C. Microbial deterioration of stone monuments—An updated overview. Adv Appl Microbiol. 2009;66:97–139.
15. Warscheid T, Braams J. Biodeterioration of stone: A review. Int Biodeter Biodegr. 2000;46:343–368.
16. Parnasa R, Nagar E, Sendersky E, et al. Small secreted proteins enable biofilm development in the cyanobacterium *Synechococcus elongatus*. Sci Rep. 2016;6:32209.
17. Parnasa R, Sendersky E, Simkovsky R, Ben-Asher HW, Golden SS, Schwarz R. A microcin processing peptidase-like protein of the cyanobacterium *Synechococcus elongatus* is essential for secretion of biofilm-promoting proteins. Environ Microbiol Rep. 2019;11:456–463.
18. Allen R, Rittmann BE, Curtiss R 3rd. Axenic biofilm formation and aggregation by synechocystis sp. Strain pcc 6803 are induced by changes in nutrient concentration and require cell surface structures. Appl Environ Microbiol. 2019;85:e02192–e02118.
19. Nagar E, Zilberman S, Sendersky E, et al. Type 4 pili are dispensable for biofilm development in the cyanobacterium *Synechococcus elongatus*. Environ Microbiol. 2017;19:2862–2872.
20. Taton A, Erikson C, Yang Y, et al. The circadian clock and darkness control natural competence in cyanobacteria. Nat Commun. 2020;11:1688.
21. Craig L, Forest KT, Maier B. Type iv pili: Dynamics, biophysics and functional consequences. Nat Rev Microbiol. 2019;17: 429–440.
22. Ellison CK, Dalia TN, Vidal Ceballos A, et al. Retraction of DNA-bound type iv competence pili initiates DNA uptake during natural transformation in vibrio cholerae. Nat Microbiol. 2018;3:773–780.
23. Schubert M, Labudde D, Oschkinat H, Schmieder P. A software tool for the prediction of xaa-pro peptide bond conformations in proteins based on 13c chemical shift statistics. J Biomol NMR. 2002;24:149–154.
24. Grzesiek S, Anglister J, Bax A. Correlation of backbone amide and aliphatic side-chain resonances in 13c/15n-enriched proteins by isotropic mixing of 13c magnetization. J Magnet Reson. 1993;B101:114–119.
25. Shen Y, Bax A. Prediction of xaa-pro peptide bond conformation from sequence and chemical shifts. J Biomol NMR. 2010; 46:199–204.
26. Schwieters CD, Kuszewski JJ, Clore GM. Using XPLOR–NIH for NMR molecular structure determination. Prog Nucl Magnet Reson Spectrosc. 2006;48:47–62.
27. Shen Y, Bax A. Protein backbone and sidechain torsion angles predicted from NMR chemical shifts using artificial neural networks. J Biomol NMR. 2013;56:227–241.
28. Kabsch W, Sander C. Dictionary of protein secondary structure: Pattern recognition of hydrogen-bonded and geometrical features. Biopolymers. 1983;22:2577–2637.
29. Lewis TE, Sillitoe I, Dawson N, et al. Gene3d: Extensive prediction of globular domains in proteins. Nucleic Acids Res. 2018; 46:D1282.
30. Berjanskii MV, Wishart DS. A simple method to predict protein flexibility using secondary chemical shifts. J Am Chem Soc. 2005;127:14970–14971.
31. Wilkins MR, Gasteiger E, Bairoch A, et al. Protein identification and analysis tools in the expasy server. Methods Mol Biol. 1999;112:531–552.
32. Fraczkiewicz R, Braun W. Exact and efficient analytical calculation of the accessible surface areas and their gradients for macromolecules. J Comput Chem. 1998;19:319–333.
33. Baker NA, Sept D, Joseph S, Holst MJ, McCammon JA. Electrostatics of nanosystems: Application to microtubules and the ribosome. Proc Natl Acad Sci U S A. 2001;98:10037–10041.

34. Krissinel E, Henrick K. Inference of macromolecular assemblies from crystalline state. J Mol Biol. 2007;372:774–797.
35. Holm L. Dali and the persistence of protein shape. Protein Sci. 2020;29:128–140.
36. Holm L, Kääriäinen S, Wilton C, Plewczynski D. Using dali for structural comparison of proteins. Curr Protoc Bioinformatics. 2006;14:5.5.1–5.5.24.
37. Cavanagh J, Fairbrother WJ, Palmer IIIAG, Skelton NJ. Protein NMR spectroscopy: Principles and practice, San Diego, CA: Elsevier, 1995.
38. Yamazaki T, Forman-Kay JD, Kay LE. Two-dimensional NMR experiments for correlating $^{13}C\beta$ and $^{1}H\delta/\varepsilon$ chemical shifts of aromatic residues in 13c-labeled proteins via scalar couplings. J Am Chem Soc. 1993;115:11054–11055.
39. Delaglio F, Grzesiek S, Vuister GW, Zhu G, Pfeifer J, Bax A. Nmrpipe: A multidimensional spectral processing system based on unix pipes. J Biomol NMR. 1995;6:277–293.
40. Lee W, Tonelli M, Markley JL. Nmrfam-sparky: Enhanced software for biomolecular nmr spectroscopy. Bioinformatics. 2015; 31:1325–1327.
41. Bhattacharya A, Tejero R, Montelione GT. Evaluating protein structures determined by structural genomics consortia. Proteins. 2007;66:778–795.
42. Laskowski RA, MacArthur MW, Moss DS, Thornton JM. Procheck: A program to check the stereochemical quality of protein structures. J Appl Cryst. 1993;26:283–291.
43. Chen VB, Arendall WB 3rd, Headd JJ, et al. Molprobity: All-atom structure validation for macromolecular crystallography. Acta Cryst. 2010;D66:12–21.
44. Sanner MF, Olson AJ, Spehner JC. Reduced surface: An efficient way to compute molecular surfaces. Biopolymers. 1996; 38:305–320.
45. Goddard TD, Huang CC, Meng EC, et al. UCSF ChimeraX: Meeting modern challenges in visualization and analysis. Protein Sci. 2018;27:14–25.

SUPPORTING INFORMATION

Additional supporting information may be found online in the Supporting Information section at the end of this article.

How to cite this article: Zhang N, Chang Y-G, Tseng R, Ovchinnikov S, Schwarz R, LiWang A. Solution NMR structure of Se0862, a highly conserved cyanobacterial protein involved in biofilm formation. *Protein Science*. 2020;29: 2274–2280. https://doi.org/10.1002/pro.3952

SUPPLEMENTARY MATERIAL

Solution NMR structure of Se0862, a highly conserved cyanobacterial protein involved in biofilm formation

Ning Zhang[1], Yong-Gang Chang[1#], Roger Tseng[1†], Sergey Ovchinnikov[2], Rakefet Schwarz[3], Andy LiWang[1,4,5*]

Authors Institutional Affiliations

[1] Department of Chemistry and Chemical Biology, University of California, Merced, CA 95343, USA

[2]Harvard University, Northwest Building 52 Oxford St. #365.20 Cambridge, MA 02138, USA

[3]The Mina and Everard Goodman Faculty of Life Sciences, Bar-Ilan University, Ramat-Gan, Israel, 5290002

[4]Center for Cellular and Biomolecular Machines, University of California, Merced, CA 95343, USA

[5]Health Sciences Research Institute, University of California, Merced, CA 95343, USA

***Corresponding Author**

Email: aliwang@ucmerced.edu

Telephone: (209) 777-6341

Current addresses:

[†]United States Department of Agriculture, Des Moines, IA 50010, USA

[#]Monash University, Victoria 3800, Australia

CONTENTS

Cloning, expression, and purification of Se0862 for NMR experiments

The gene fusion for SUMO-Se0862 was cloned into pET-28b as specified in Table S4. The fusion protein was overexpressed in *E. coli* BL21 (DE3) cells. For NMR sample preparation, cells were grown at 37 °C in M9 minimal medium containing $^{15}NH_4Cl$ and uniformly ^{13}C-labeled D-glucose as the sole sources of nitrogen and carbon, respectively. Protein overexpression was initiated by adding 0.2 mM isopropyl β-d-1-thiogalactopyranoside (IPTG) when cell cultures reached an OD_{600} of ~0.5. After ~12 h at 30 °C cells were harvested by centrifugation (8 min at 4 °C, 5,000 rpm). Cell pellets were resuspended in lysis buffer (50 mM NaH_2PO_4, 500 mM NaCl, pH 8.0) and subsequently lysed by an Avestin EmulsiFlex-C3 homogenizer (Avestin Inc., Canada). The supernatant was loaded on Ni-NTA columns equilibrated with lysis buffer. Five column volumes of wash buffer (50 mM NaH_2PO_4, 500 mM NaCl, 20 mM imidazole, pH 8.0) were applied to the column. The SUMO-Se0862 fusion protein was then eluted with 50 mM NaH_2PO_4, 500 mM NaCl, 250 mM imidazole, pH 8.0 and subjected to ULP1 protease digestion overnight at 4 °C. The His-tagged SUMO protein and ULP1 were removed by a second Ni-NTA chromatography step. The flow-through fraction from this second column was concentrated and loaded on a HiLoad Superdex 75 16/600 column (GE Healthcare, USA) equilibrated with buffer (20 mM Tris, 100 mM NaCl, pH 7.0). The molecular mass of Se0862 was approximated by gel-filtration analysis to be 15.5 kDa, which when compared to the sequence-derived mass of 14.4 kDa suggests that Se0862 is monomer in solution (Figure S1). The purity of Se0862 samples as estimated from SDS-PAGE was ~99%. Figure S1 provides a flowchart that summarizes cloning, overexpression, and purification of Se0862.

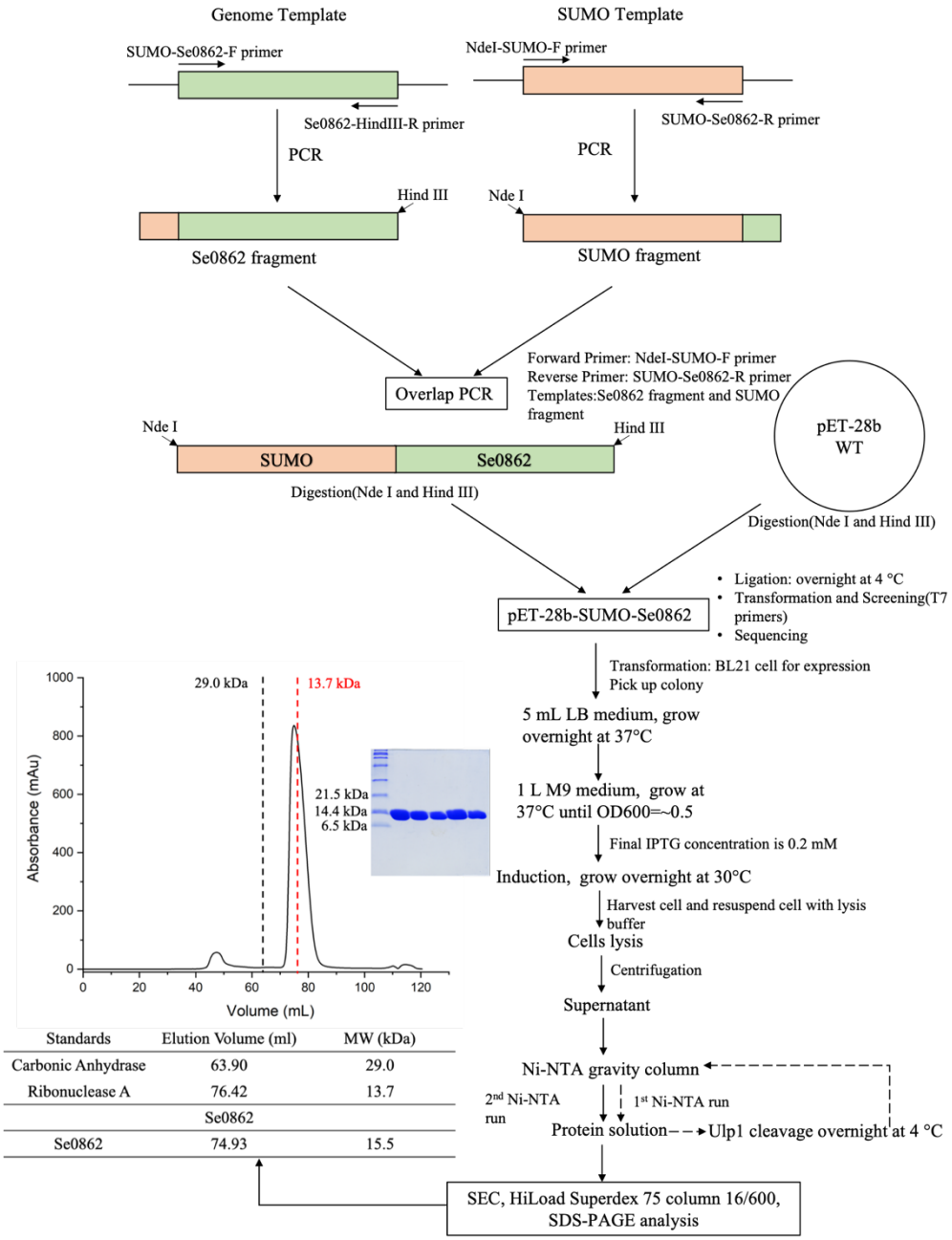

Figure S1. Flowchart for gene cloning, protein expression, and purification of Se0862. Black and red dash lines represent standard proteins, carbonic anhydrase and ribonuclease A, respectively, which were used for calibrating the preparative size-exclusion column. The elution volume of Se0862 corresponded to approximately 15.5 kDa, as compared to 14.4 kDa, which is its molecular weight calculated from the amino acyl sequence.

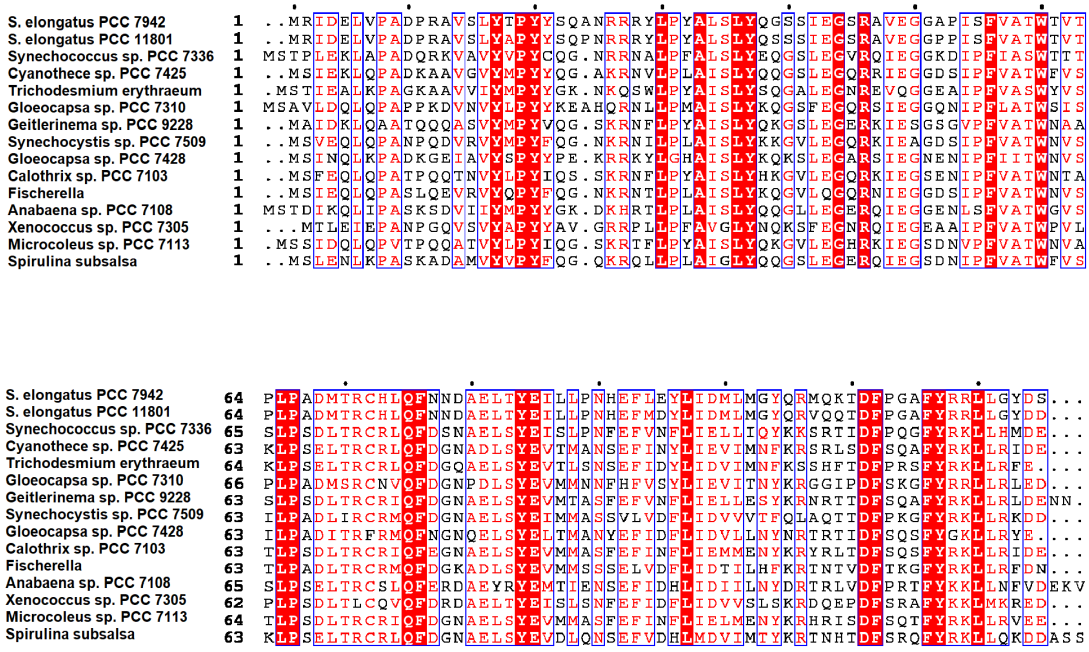

Figure S2. Se0862 is a hypothetical protein that is highly conserved in diverse cyanobacteria.

Identical residues are shaded red, similar amino acids have red type, and segments of similarity are enclosed by blue boxes. Every 10th residue is marked by a black dot. NCBI accession numbers are as follows: *S. elongatus* PCC 7942: WP_011242990.1; *S. elongatus* PCC 11801: AZB72417.1; *Synechococcus sp.* PCC 7336: WP_071515349.1; *Cyanothece sp.* PCC 7425: WP_015185783.1; *Trichodesmium erythraeum*: WP_006507693.1; *Gloeocapsa sp.* PCC 7310: WP_012625922.1; *Geitlerinema sp.* PCC 9228: WP_019492979.1; *Synechocystis sp.* PCC 7509: WP_009633946.1; *Gloeocapsa sp.* PCC 7428: WP_011612292.1; *Calothrix sp.* PCC 7103: WP_009457513.1; *Fischerella*: WP_015189180.1; *Anabaena sp.* PCC 7108: WP_006528876.1; *Xenococcus sp.* PCC 7305: WP_017325253.1; *Microcoleus sp.* PCC 7113: WP_016951792.1; *Spirulina subsalsa*: WP_017304516.1.

Table S1. Prolyl residues in Se0862 are *trans* based on ^{13}C chemical shift differences.

Prolines	δC_β (ppm)	δC_γ (ppm)	$\Delta_{\beta\gamma} = \delta C_\beta - \delta C_\gamma$ (ppm)	P-*cis*∗
P8	31.76	27.26	4.50	0.01
P11	32.40	27.29	5.11	0.00
P19	31.38	27.78	3.60	0.00
P31	31.38	28.84	2.54	0.00
P53	32.43	27.30	5.13	0.02
P64	33.26	27.64	5.62	0.00
P66	33.25	27.63	5.62	0.00
P89	32.74	28.19	4.55	0.00
P113	32.25	28.74	3.51	0.00

*P-*cis* is the probability of a prolyl residue to adopt the *cis* conformation. P-*cis* values were calculated by the Promega server.

Table S2. The top 20 DALI-matched structural homologs of Se0862.

PDB	Z-score	RMSD	Description
1UKF-A	3.4	3.1	AVIRULENCE PROTEIN AVRPPHB
4RGI-A	3.2	3.3	UNCHARACTERIZED PROTEIN
4A0G-A	3.2	5.7	ADENOSYLMETHIONINE-8-AMINO-7-OXONONANOATE
4KQE-A	3.2	4.2	GLYCYL-TRNA SYNTHETASE
2FFG-A	3.1	3.2	YKUJ
2RA8-A	3.1	2.6	UNCHARACTERIZED PROTEIN Q64V53_BACFR
6PGV-A	3	2.9	JOSEPHIN-2
5D16-A	3	5.6	TRANSPOSON TN7 TRANSPOSITION PROTEIN TNSE
2W9J-B	2.9	3	SIGNAL RECOGNITION PARTICLE SUBUNIT SRP14
2OQB-A	2.8	8.3	HISTONE-ARGININE METHYLTRANSFERASE CARM1
3HSA-A	2.8	4.6	PLECKSTRIN HOMOLOGY DOMAIN
4DMO-A	2.8	3.1	N-HYDROXYARYLAMINE O-ACETYLTRANSFERASE
4FBJ-A	2.8	3.3	HYPOTHETICAL PROTEIN
2WZO-A	2.7	4.8	TRANSFORMING GROWTH FACTOR BETA REGULATOR 1
6NF1-A	2.7	8.7	PROTO-ONCOGENE VAV
6E8A-A	2.6	7.8	DUF1795 DOMAIN-CONTAINING PROTEIN
6EGT-A	2.6	3.7	GLYCOPROTEIN
4NCJ-A	2.6	4.7	DNA DOUBLE-STRAND BREAK REPAIR RAD50 ATPASE
2ZT7-A	2.6	4.1	GLYCYL-TRNA SYNTHETASE
4DDG-A	2.6	4.9	UBIQUITIN-CONJUGATING ENZYME E2 D2, UBIQUITIN THI

Table S3. NMR experimental conditions for Se0862.

Samples	NMR experiments	Experimental conditions
$^{15}N/^{13}C$-enriched Se0862	$^{1}H/^{15}N$-HSQC	• Volume: 350 µL • ^{1}H /^{15}N sweep widths (Hz): 9615.385/ 1827.578 • ^{1}H /^{15}N acquisition times (ms): 67.912/54.717 • ^{1}H /^{15}N carrier frequencies (ppm): 4.871/ 119.694 • Temperature: 22 °C • Protein concentration: ~600 µM • Buffer: 20 mM Tris, 100 mM NaCl, 5 mM TCEP, 0.02% NaN_3, 10 µM DSS, pH 7.0, 95% H_2O/5% D_2O • NMR tube: Bruker Shaped Tube
	3D HNCACB 3D HN(CO)CACB	• Volume: 350 µL • ^{1}H /^{15}N /^{13}C sweep widths (Hz): 9615.385/ 1583.899/9500.00 • ^{1}H /^{15}N /^{13}C acquisition times (ms): 69.888/ 23.991/7.053 • ^{1}H /^{15}N /^{13}C carrier frequencies (ppm): 4.833/ 119.654/46.00 • Temperature: 22 °C • Protein concentration: ~600 µM • Buffer: 20 mM Tris, 100 mM NaCl, 5 mM TCEP, 0.02% NaN_3, 10 µM DSS, pH 7.0, 95% H_2O/5% D_2O • NMR tube: Bruker Shaped Tube
	3D HN(CA)CO 3D HNCO	• Volume: 350 µL • ^{1}H /^{15}N /^{13}C sweep widths (Hz): 9615.385/ 1583.899/1500.00 • ^{1}H /^{15}N /^{13}C acquisition times (ms): 69.888/ 23.360/30.000 • ^{1}H /^{15}N /^{13}C carrier frequencies (ppm): 4.833/ 119.654/176.00 • Temperature: 22 °C • Protein concentration: ~600 µM • Buffer: 20 mM Tris, 100 mM NaCl, 5 mM TCEP, 0.02% NaN_3, 10 µM DSS, pH 7.0, 95% H_2O/5% D_2O • NMR tube: Bruker Shaped Tube

	3D HBHA(CO)NH	• Volume: 350 µL • ^{1}H /^{15}N /^{1}H sweep widths (Hz): 9615.385/ 1583.899/4000.00 • ^{1}H /^{15}N /^{1}H acquisition times (ms): 69.888/23.991/13.000 • ^{1}H /^{15}N /^{1}H carrier frequencies (ppm): 4.833/ 119.654/4.833 • Temperature: 22 °C • Protein concentration: ~600 µM • Buffer: 20 mM Tris, 100 mM NaCl, 5 mM TCEP, 0.02% NaN_3, 10 µM DSS, pH 7.0, 95% H_2O/5% D_2O • NMR tube: Bruker Shaped Tube
	3D HCCH(CO)NH	• Volume: 350 µL • ^{1}H /^{15}N /^{1}H sweep widths (Hz): 9615.385/ 1583.899/4000.000 • ^{1}H /^{15}N /^{1}H acquisition times (ms): 67.912/ 23.991/13.000 • ^{1}H /^{15}N /^{1}H carrier frequencies (ppm): 4.871/ 119.694/4.871 • Temperature: 22 °C • Protein concentration: ~600 µM • Buffer: 20 mM Tris, 100 mM NaCl, 5 mM TCEP, 0.02% NaN_3, 10 µM DSS, pH 7.0, 95% H_2O/5% D_2O • NMR tube: Bruker Shaped Tube
	3D CC(CO)NH	• Volume: 350 µL • ^{1}H /^{15}N /^{13}C sweep widths (Hz): 9615.385/ 1583.899/9674.291 • ^{1}H / ^{15}N / ^{13}C acquisition times (ms): 67.912/ 23.991/8.063 • ^{1}H /^{15}N /^{13}C carrier frequencies (ppm): 4.872/ 119.194/46.094 • Temperature: 22 °C • Protein concentration: ~600 µM • Buffer: 20 mM Tris, 100 mM NaCl, 5 mM TCEP, 0.02% NaN_3, 10 µM DSS, pH 7.0, 95% H_2O/5% D_2O • NMR tube: Bruker Shaped Tube

	2D (HB)CB(CDCG)HG	• Volume: 350 µL • ^{1}H /^{13}C sweep widths (Hz): 9615.385/ 6046.364 • ^{1}H /^{13}C acquisition times (ms): 49.92/8.10 • ^{1}H /^{13}C carrier frequencies (ppm): 4.70/32.00 • Temperature: 22 °C • Protein concentration: ~600 µM • Buffer: 20 mM Tris, 100 mM NaCl, 5 mM TCEP, 0.02% NaN_3, 10 µM DSS, pH 7.0, 95% H_2O/5% D_2O • NMR tube: Bruker Shaped Tube
	2D (HB)CB(CDCGCE)HE	• Volume: 350 µL • ^{1}H /^{13}C sweep widths (Hz): 9615.385/ 6046.364 • ^{1}H /^{13}C acquisition times (ms): 49.92/8.10 • ^{1}H /^{13}C carrier frequencies (ppm): 4.70/32.16 • Temperature: 22 °C • Protein concentration: ~600 µM • Buffer: 20 mM Tris, 100 mM NaCl, 5 mM TCEP, 0.02% NaN_3, 10 µM DSS, pH 7.0, 95% H_2O/5% D_2O • NMR tube: Bruker Shaped Tube
^{15}N/^{13}C-enriched Se0862 in 5.2% stretched polyacrylamide gel (alignment medium)	3D IPAP-J-HNCO ^{1}J(N-H)	• Volume: 350 µL (isotropic sample); 600 µL (anisotropic sample) • ^{1}H /^{13}C /^{15}N sweep widths (Hz): 7211.539/ 1500.004/1583.899 • ^{1}H /^{13}C /^{15}N acquisition times (ms): 67.95/ 20.00/46.72 • ^{1}H /^{13}C /^{15}N carrier frequencies (ppm): 4.852/ 176.074/119.674 • Temperature: 22 °C • Protein concentration: ~500 µM • Buffer: 20 mM Tris, 100 mM NaCl, 5 mM TCEP, 0.02% NaN_3, 10 µM DSS, pH 7.0, 95% H_2O/5% D_2O • NMR tube: Bruker Shaped Tube (isotropic sample); 4.2 mm New Era NMR tubes (NE-UP5-GT-7) (anisotropic sample)

	3D IPAP-J-HNCO ^{1}J(CA-HA)	• Volume: 350 µL (isotropic sample); 600 µL (anisotropic sample) • ^{1}H /^{13}C /^{15}N sweep widths (Hz): 7211.539/ 1500.000/1583.899 • ^{1}H /^{13}C / ^{15}N acquisition times (ms): 67.95/ 50.67/23.36 • ^{1}H /^{13}C /^{15}N carrier frequencies (ppm): 4.852/ 176.074/119.674 • Temperature: 22 °C • Protein concentration: ~500 µM • Buffer: 20 mM Tris, 100 mM NaCl, 5 mM TCEP, 0.02% NaN_3, 10 µM DSS, pH 7.0, 95% H_2O/5% D_2O • NMR tube: Bruker Shaped Tube (isotropic sample); 4.2 mm New Era NMR tubes (NE-UP5-GT-7) (anisotropic sample)
	3D IPAP-J-HNCO ^{1}J(CA-CO)	• Volume: 350 µL (isotropic sample); 600 µL (anisotropic sample) • ^{1}H /^{13}C /^{15}N sweep widths (Hz): 7211.539/ 1500.000/1583.899 • ^{1}H /^{13}C / ^{15}N acquisition times (ms): 67.95/ 50.67/23.36 • ^{1}H /^{13}C /^{15}N carrier frequencies (ppm): 4.852/ 176.074/119.674 • Temperature: 22 °C • Protein concentration: ~500 µM • Buffer: 20 mM Tris, 100 mM NaCl, 5 mM TCEP, 0.02% NaN_3, 10 µM DSS, pH 7.0, 95% H_2O/5% D_2O • NMR tube: Bruker Shaped Tube (isotropic sample); 4.2 mm New Era NMR tubes (NE-UP5-GT-7) (anisotropic sample)
^{15}N/^{13}C-enriched Se0862	3D ^{15}N-NOESY-HSQC	• Volume: 350 µL • ^{1}H /^{15}N /^{1}H sweep widths (Hz): 9615.385/ 1949.416/6011.328 • ^{1}H /^{15}N /^{1}H acquisition times (ms): 67.912/ 20.519/24.953 • ^{1}H /^{15}N /^{1}H carrier frequencies (ppm): 4.779/ 119.601/4.779 • Mixing Time: 80 ms

		• Temperature: 22 °C • Protein concentration: ~600 µM • Buffer: 20 mM Tris, 100 mM NaCl, 5 mM TCEP, 0.02% NaN_3, 10 µM DSS, pH 7.0, 95% H_2O/5% D_2O • NMR tube: Bruker Shaped Tube
^{13}C-enriched Se0862 in D_2O	$^{1}H/^{13}C$-HSQC Full spectrum	• Volume: 350 µL • ^{1}H /^{13}C sweep widths (Hz): 7211.539/ 10581.219 • ^{1}H /^{13}C acquisition times (ms): 49.920/23.249 • ^{1}H /^{13}C carrier frequencies (ppm): 2.877/ 43.809 • Temperature: 22 °C • Protein concentration: ~600 µM • Buffer: 20 mM Tris, 100 mM NaCl, 5 mM TCEP, 0.02% NaN_3, 10 µM DSS, pD 7.0, 99.96% D_2O • NMR tube: Bruker Shaped Tube
	$^{1}H/^{13}C$-HSQC Folded spectrum	• Volume: 350 µL • ^{1}H /^{13}C sweep widths (Hz): 7211.539/ 4534.813 • ^{1}H /^{13}C acquisition times (ms): 49.920/46.749 • ^{1}H /^{13}C carrier frequencies (ppm): 2.877/ 42.559 • Temperature: 22 °C • Protein concentration: ~600 µM • Buffer: 20 mM Tris, 100 mM NaCl, 5 mM TCEP, 0.02% NaN_3, 10 µM DSS, pD 7.0, 99.96% D_2O • NMR tube: Bruker Shaped Tube
	3D ^{13}C-NOESY-HSQC	• Volume: 350 µL • ^{1}H /^{13}C /^{1}H sweep widths (Hz): 7211.539/ 4534.808/5410.185 • ^{1}H /^{13}C /^{1}H acquisition times (ms): 49.920/ 9.04/20.332 • ^{1}H /^{13}C /^{1}H carrier frequencies (ppm): 2.877/ 42.577/2.877 • Mixing Time: 80 ms • Temperature: 22 °C • Protein concentration: ~600 µM

		• Buffer: 20 mM Tris, 100 mM NaCl, 5 mM TCEP, 0.02% NaN_3, 10 µM DSS, pD 7.0, 99.96% D_2O • NMR tube: Bruker Shaped Tube
	3D ^{13}C-(H)CCH-COSY	• Volume: 350 µL • ^{1}H /^{13}C /^{13}C sweep widths (Hz): 7211.539/ 4534.808/4534.808 • ^{1}H /^{13}C /^{13}C acquisition times (ms): 49.920/ 9.04/9.04 • ^{1}H /^{13}C /^{13}C carrier frequencies (ppm): 2.877/ 42.577/42.577 • Temperature: 22 °C • Protein concentration: ~600 µM • Buffer: 20 mM Tris, 100 mM NaCl, 5 mM TCEP, 0.02% NaN_3, 10 µM DSS, pD 7.0, 99.96% D_2O • NMR tube: Bruker Shaped Tube
	3D ^{13}C-H(C)CH-COSY	• Volume: 350 µL • ^{1}H /^{13}C /^{1}H sweep width (Hz): 7211.539/ 4534.808/5410.185 • ^{1}H /^{13}C /^{1}H acquisition time (ms): 49.920/ 9.04/20.332 • ^{1}H /^{13}C /^{1}H carrier frequencies (ppm): 3.00/ 43.00/3.00 • Temperature: 22 °C • Protein concentration: ~600 µM • Buffer: 20 mM Tris, 100 mM NaCl, 5 mM TCEP, 0.02% NaN_3, 10 µM DSS, pD 7.0, 99.96% D_2O • NMR tube: Bruker Shaped Tube
	3D ^{13}C-(H)CCH-TOCSY	• Volume: 350 µL • ^{1}H /^{13}C /^{13}C sweep widths (Hz):7211.539/ 4534.806/4534.806 • ^{1}H /^{13}C /^{13}C acquisition times (ms): 49.920/ 9.04/9.04 • ^{1}H /^{13}C /^{13}C carrier frequencies (ppm): 3.00/ 43.00/43.00 • Temperature: 22 °C • Protein concentration: ~600 µM

		• Buffer: 20 mM Tris, 100 mM NaCl, 5 mM TCEP, 0.02% NaN_3, 10 µM DSS, pD 7.0, 99.96% D_2O • NMR tube: Bruker Shaped Tube
	4D ^{13}C /^{13}C-edited-NOESY-HSQC	• Volume: 350 µL • ^{1}H /^{13}C /^{1}H /^{13}C sweep widths (Hz): 7211.539/ 4534.806/5410.188/4534.806 • ^{1}H /^{13}C /^{1}H /^{13}C acquisition times (ms): 49.920/3.528/8.133/3.528 • ^{1}H /^{13}C /^{1}H /^{13}C carrier frequencies (ppm): 3.00/43.00/3.00/43.00 • Mixing Time: 80 ms • Temperature: 22 °C • Protein concentration: ~600 µM • Buffer: 20 mM Tris, 100 mM NaCl, 5 mM TCEP, 0.02% NaN_3, 10 µM DSS, pD 7.0, 99.96% D_2O • NMR tube: Bruker Shaped Tube

pD = pH + 0.4, where pH was the uncorrected meter reading of 6.6 for the 99.96% D_2O NMR samples[1].

Table S4. Primers and M9 minimal media used in this study.

Primers for Se0862-containing recombinant plasmid (pET-28b-6xHis-SUMO- Se0862)	
Primer Name	Primer Sequence (5' →3')
NdeI-SUMO-F	GGGAATTCCATATGGCTAGCATGTCGGACTCAGAAGTCAATC
SUMO- Se0862-F	ACAGAGAACAGATTGGTGGAATGCGAATTGATGAACTGGT
SUMO- Se0862-R	ACCAGTTCATCAATTCGCATTCCACCAATCTGTTCTCTGT
Se0862-HindIII-R	CCCAAGCTTTCAGCTGTCGTAACCCAGCAATC

M9 minimal media for NMR sample preparation (1 L volume)

^{13}C-only media	^{15}N/^{13}C media
Na_2HPO_4 (6.0 g)	Na_2HPO_4 (6.0 g)
KH_2PO_4 (3.0 g)	KH_2PO_4 (3.0 g)
NaCl (0.5 g)	NaCl (0.5 g)
$MgSO_4$ (2 mM)	$MgSO_4$ (2 mM)
$CaCl_2$ (100 μM)	$CaCl_2$ (100 μM)
$^{13}C_6$-D-Glucose (2.0 g)	$^{13}C_6$-D-Glucose (2.0 g)
NH_4Cl (1.0 g)	$^{15}NH_4Cl$ (1.0 g)

REFERENCE

1. Covington AK, Paabo M, Robinson RA, Bates RG. 1968. Use of the glass electrode in deuterium oxide and the relation between the standardized pD (pa_D) scale and the operational pH in heavy water. *Analytical Chemistry*. 40:700-706.